Available online at http://scik.org
Commun. Math. Biol. Neurosci. 2026, 2026:84
https://doi.org/10.28919/cmbn/10072
ISSN: 2052-2541

GLOBAL STABILITY ANALYSIS OF A NEW MULTISCALE HBV MODEL WITH THERAPY

ISMAIL AAMOUM[1,*], ADIL MESKAF[1,2]

[1]Experimental Laboratory of Innovation in Technology and Simulations, Chouaib Doukkali university, El Jadida, Morocco

[2]Department of SEG, Faculty of Economic and Social Legal Sciences, Chouaib Doukkali university, El Jadida, Morocco

Abstract. This paper discusses the viral dynamics of hepatitis B virus with a new multi-scale model. The model studies the interaction between hepatitis B virus (HBV) and liver cells (hepatocytes) with the presence of two types of therapy. The first represents the efficacy of the treatment drug in preventing new infections, while the second represents the efficacy of the drug treatment in inhibiting viral production. The equilibrium points of the model are well defined, their global stability has been studied and the basic reproduction rate has been calculated. Finally, numerical simulations are established to confirm our theoretical results.

Keywords: multiscale model; global stability; HBV; Lyapunov function.

2020 AMS Subject Classification: 92C60.

1. INTRODUCTION

As a result of viral infection, viral hepatitis causes inflammation of the liver.[1]. Those infections include hepatitis B virus (HBV) and hepatitis C virus (HCV), as well as hepatitis D virus and hepatitis E virus. Millions of individuals are infected with viral hepatitis every year,

*Corresponding author

E-mail address: aamoum.ismail@ucd.ac.ma

Received June 19, 2026

which is a serious public health concern. Some infections eventually result in hepatocellular carcinoma (HCC), liver cirrhosis, and mortality in a sizeable number of patients[2]. There are significant morbidities and mortality associated with hepatitis B, one of the most common and severe infectious diseases [3]. A third of people on the planet are thought to have HBV infection. A quarter of those who are chronic carriers—about 5% of this population—develop significant liver illnesses such cirrhosis, hepatic cancer, and chronic hepatitis. [4].Around the world, 780000 HBV-related deaths are reported each year[4]. The disease rate for HBV is high among the sub-Saharan population. Infection with HBV affects around 6.1% of Africans, while chronic HCV infection affects over 18 million people[2].

The hepatitis B virus (HBV) belongs to the family of Hepadnaviridae, which comprises hepatotropic DNA viruses. Its highly ordered, circular, partly double-stranded DNA genome makes it distinctive[5, 6]. Upon entering the hepatocyte and subsequent placement into the nucleus, covalently closed circular DNA (cccDNA) is transformed by host cell repair mechanisms into relaxed circular DNA[7, 8]. A cccDNA is transcribed by host cell mechanisms into subgenomic and pregenomic RNA (pgRNA), which is then further processed. Following encapsidation, viral reverse transcriptase generates genomic DNA from the pgRNA binds specifically to viral core proteins in the cytoplasm. [9]. The resultant capsids have two options: they may either re-enter the nucleus to maintain the reservoir of viral cccDNA templates inside the host cell, or they can be encased and expelled as new virions [5, 10]. The host cell produces RNA templates of the supercoiled viral cccDNA during normal protein biosynthesis, and depending on the open reading frame (ORF), these RNA templates are translated into one of the seven proteins listed below[11, 12].

Unfortunately, HBV cannot be cured with current therapy.[13]. Interferon and nucleosidic reverse transcriptase inhibitors are now used as conventional treatments. Further, approaches for developing targeted therapies and substances with unique modes of action are discussed[13].

Over the past few decades, mathematical modeling has emerged as an indispensable tool for understanding the transmission dynamics of infectious diseases and evaluating the efficacy

of control strategies. Pioneer studies have successfully applied compartmental models to investigate various pathodynamic systems, such as COVID-19 transmission patterns under non-pharmaceutical interventions [14, 15] and the co-infection dynamics of HIV and tuberculosis [16]. Furthermore, mathematical formulations incorporating spatial diffusion and fractional-order derivatives have been deployed to analyze the intra-host dynamics of viral infections like influenza [17]. Building upon these computational and theoretical frameworks, applying mathematical models to the Hepatitis B Virus (HBV) provides critical insights into chronic infection mechanisms, immune responses, and optimal therapeutic interventions.

Mathematical modelling has a very large role in understanding the dynamics of hepatitis B virus. The basic model that analyzes the effect of antivirus in reducing viral load was presented in 1996 by Nowak et al [18]. Other models studied the interaction between antiviral treatment and HBV [18, 19, 20, 21, 35, 36, 37, 38, 39, 40, 41, 42]. In addition, there are models that have studied the effect of delay in time or spatial diffusion [22, 23, 24, 25, 26]. In addition, some models are used to understand the interaction between hepatocytes infected with cccDNA [27, 28].

However, these cited models cannot describe the intracellular viral dynamics that are necessary to complement the various antiviral effects corresponding to the action mechanisms of drugs. Some papers have presented multiscale models that take into account the dynamics of intracellular viral replication [29, 30]. These multiscale models were constructed using partial differential equations (EDP), but Kitagawa et al. [31] introduced a new approach that transforms a multiple-scale standard model of HCV infection into an equivalent system of ordinary differential equations (EDEs) without assumptions. In this work, we will present a new mathematical model described the interaction between the transformed multiscale model of the HBV infection in ODE form and antiviral effects of multi-drug treatments by defining three efficacies. The model helps improve our understanding of HBV-drug interactions treatments and infected hepatocytes. In section 2, the multiscale model's ODE model is used to characterize the dynamics of the HBV infection. Section 3 presents a conditions for positivity of the extanded model and his basic reproduction number. Section 4 determines the equilibrium points, Section 5 presents

the stability analysis and in section 6 we present some numerical simulations. Finally, section 7 concludes the paper.

2. THE TRANSFORMED MULTISCALE ODE HBV MODEL

Many authors describe the intracellular life cycle with a multiscale model in the form of PDEs [29, 32, 30]. The model is presented as follows:

$$\frac{\partial R(a,t)}{\partial t} + \frac{\partial R(a,t)}{\partial a} = \alpha(1-\varepsilon_\alpha) - ((1-\varepsilon_s)\rho + k\mu))R(a) \tag{1}$$

$$\frac{dT(t)}{dt} = s - rT(t) - \beta V(t)T(t) \tag{2}$$

$$\frac{\partial i(a,t)}{\partial t} + \frac{\partial i(a,t)}{\partial a} = -\delta i(a,t) \tag{3}$$

$$\frac{dV(t)}{dt} = (1-\varepsilon_s)\rho \int_0^\infty R(a,t)i(a,t)\,da - cV(t) \tag{4}$$

$T(t)$ is the target cells that reproduce at rate s and die at rate r and be infected by viruses with a rate β. $V(t)$ is the number of the viruses. $i(a,t)$ is the age distribution of infected cells, $R(a,t)$ represents the age distribution of intracellular viral RNA in cell with age a that reproduce at rate α and be degraded at rate μ. The infected cells die at rate δ and virions are cleared at rate c. ρ represents the rate which RNA assemble and be secreted from an infected cell. Three efficacies of the antiviral effect of treatment are considered; ε_s, ε_α and k.

In this work, we introduce a new multiscale HBV model with therapy based in the transformed multiscale model into an ODE model that presented by Kitagawa et al. [31].

Hence, the proposed model is described by the following ODEs system:

$$\frac{dH(t)}{dt} = s - rH(t) - \beta V(t)H(t) \tag{5}$$

$$\frac{dI(t)}{dt} = \beta V(t)H(t) - \delta I(t) \tag{6}$$

$$\frac{dP(t)}{dt} = \beta V(t)H(t) + \alpha(1-\varepsilon_\alpha)I(t) - (k\mu + \rho(1-\varepsilon_s) + \delta)P(t) \tag{7}$$

$$\frac{dV(t)}{dt} = \rho(1-\varepsilon_s)P(t) - cV(t) \tag{8}$$

Where H denotes the healthy hepatocytes, V is the number of viruses, I describes the total number of infected hepatocytes. When the virus is imported into the hepatocyte nucleus, DNA repairs from a rcDNA to cccDNA and is transcribed to pgARN. P represent the total amount of intracellular viral pgRNA pooled in all infected cells.

3. Properties of the Transformed Model

3.1. Positivity of the solution.

Theorem 3.1. *Let $\tau > 0$, if the initial conditions are positive; $H(0) \geq 0$, $I(0) \geq 0$, $P(0) \geq 0$ and $V(0) \geq 0$, then for all $t \in [0,\tau]$, $H(t), I(t), P(t)$ and $V(t)$ will stand positive in $\mathbb{R}^4$.*

Proof. All parameters in the systeme 5-8 are positive, thus:

$$\begin{aligned}
\frac{dH(t)}{dt} &\geq -rH(t) - \beta V(t)H(t) \\
\frac{dI(t)}{dt} &\geq -\delta I(t) \\
\frac{dP(t)}{dt} &\geq -(k\mu + \rho(1-\varepsilon_s) + \delta)P(t) \\
\frac{dI(t)}{dt} &\geq -cV(t)
\end{aligned}$$

We can deal with inequality and produce:

$$\begin{aligned}
H(t) &\geq \exp(-rt - \int_0^\tau \beta V(t)\,dt) \geq 0 \\
I(t) &\geq \exp(-\delta t) \geq 0 \\
P(t) &\geq \exp(-(k\mu + \rho(1-\varepsilon_s) + \delta)t) \geq 0 \\
V(t) &\geq \exp(-ct) \geq 0
\end{aligned}$$

□

3.2. The basic reproduction number R_0.

Definition 3.1. The basic number of reproduction is defined as the number of new viral particles created over the full time of infection from one average viral particle in an uninfected cell population.

The basic number of reproduction will be calculated with no treatement; $\varepsilon_s = 0, \varepsilon_\alpha = 0$ and $k = 1$, and also at the disease-free equilibrium $E_0 = (\frac{s}{r}, 0, 0, 0)$ wich will be explain explicitly in the next section. Many approches can be used to compute R_0. In our work, we will applied the approach that is presented by Castillo-Chavez, et. al [33]. Accordingly, we consider $\Phi = (H)$, $\Psi = (I, P)$,$\gamma = (V)$, The model without treatement can be written as:

$$\frac{d\Phi}{dx} = f(\Phi, \Psi, \gamma)$$

$$\frac{d\Psi}{dx} = g(\Phi, \Psi, \gamma)$$

$$\frac{d\gamma}{dx} = h(\Phi, \Psi, \gamma)$$

The disease-free equilibrium is defined as $E_0 = (\Phi_0, \Psi_0, \gamma_0)$ such that: $\Phi_0 = (H_0)$, $\Psi_0 = (0, 0)$ and $\gamma_0 = (0)$

taking into $g(\Phi_0, \Psi, \gamma) = 0$;

$$\beta V H_0 - \delta I = 0 \quad and \quad \beta V H_0 + \alpha I - (\mu + \rho + \delta) P = 0$$

We solve these two equations for I and P as a function of V:

$$I = \frac{\beta V H_0}{\delta} \quad and \quad P = \frac{\beta H_0 (\delta + \alpha)}{\delta(\mu + \rho + \delta)} V$$

Substituting in $h(\Phi_0, I, P, V)$:

$$h(\Phi_0, I, P, V) = \rho \frac{\beta H_0 (\delta + \alpha)}{\delta(\mu + \rho + \delta)} V - cV$$

$$h(\Phi_0, I, P, V) = (\rho \frac{\beta H_0 (\delta + \alpha)}{\delta(\mu + \rho + \delta)} - c) V$$

Hence, the basic reproductive number is the spectral radius of $MD^{-}1$ such that :

$$M = \rho \frac{\beta H_0 (\delta + \alpha)}{\delta(\mu + \rho + \delta)} \quad and \quad D = c$$

Consequently,

$$R_0 = \frac{\rho \beta H_0 (\delta + \alpha)}{c\delta(\mu + \rho + \delta)} = \frac{\rho \beta s (\delta + \alpha)}{cr\delta(\mu + \rho + \delta)} \tag{9}$$

4. THE EQUILIBRIUM POINTS

Equilibrium points are values for variables H^*, I^*, P^* and V^* without treatment that satisfy:

$$s - rH^* - \beta V^* H^* = 0 \tag{10}$$

$$\beta V^* H^* - \delta I^* = 0 \tag{11}$$

$$\beta V^* H^* + \alpha I^* - (\mu + \rho + \delta) P^* = 0 \tag{12}$$

$$\rho P^* - cV^* = 0 \tag{13}$$

We obtain 2 equilibrium points :

- The virus-free equilibrium point:

$$E_0 = \left(\frac{s}{r}, 0, 0, 0\right) \tag{14}$$

- The infected equilibrium point:

$$E_1 = \left(\frac{c\delta_1}{\beta_1}, \frac{K}{\delta\beta_1}, \frac{K}{\beta\rho\delta_1}, \frac{K}{c\beta\delta_1}\right)$$

Where:

$$\begin{aligned} K &= s\beta\rho\alpha + s\beta\rho\delta - rc\delta^2 - rc\delta\mu - rc\delta\rho \\ &= s\beta\rho(\alpha+\delta) - rc\delta(\delta+\mu+\rho) \\ &= rc\delta(\delta+\mu+\rho)(R_0-1) \end{aligned}$$

$$\beta_1 = \beta\rho(\alpha+\delta)$$

$$\delta_1 = \delta(\mu+\rho+\delta)$$

Hence, the infected equilibrium point E_1 can be given as:

$$E_1 = \left(\frac{s}{rR_0}, \frac{s}{\delta}(1-\frac{1}{R_0}), \frac{rc}{\rho\beta}(R_0-1), \frac{r(R_0-1)}{\beta}\right) \tag{15}$$

As equilibrium points should have positive coordinates, E_1 exist and $E_1 \neq E_0$ if $R_0 > 1$.

5. GLOBAL STABILITY

5.1. Global stability of uninfected equilibrium point.

Theorem 5.1. *E_0 is globally asymptotically stable if $R_0 \leq 1$*

Proof. We consider a Lyapunov function for $E_0 = \left(H^0, I^0, P^0, V^0\right)$ as follow:

$$L(t) = H^0 \left(\frac{H}{H^0} - 1 - \ln\left(\frac{H}{H^0}\right)\right) + I + \frac{\delta}{\alpha} P + \frac{\delta}{\alpha\rho}(\rho + \mu + \delta)V$$

$$L(t) = H^0 \left(\frac{H}{H^0} - 1 - \ln\left(\frac{H}{H^0}\right)\right) + I + \frac{\delta}{\alpha} P + \frac{\delta}{\alpha\rho}(\rho + \mu + \delta)V$$

Hence,

$$\frac{dL(t)}{dt} = s\left(2 - \frac{H}{H^0} - \frac{H^0}{H}\right) + \frac{c\delta(\delta + \rho + \mu}{\rho\alpha}(R_0 - 1)$$

We have : $2 - \frac{H}{H^0} - \frac{H^0}{H} \leq 0$, Because the arithmetic mean exceeds the geometric mean.[34]
So, when $R_0 \leq 1$ then $\frac{dL(t)}{dt} \leq 0$.and $\frac{dL(t)}{dt} = 0$ if $H = H^0, I = P = V = 0$
We consider :M the largest invariant in $\{(H,I,P,V) / \frac{dL(t)}{dt} = 0\}$.
Thus: $M = \{E_0\}$. By the Lyapunov–LaSalle invariance principle, we deduce that E_0 is globally asymptotically stable whenever $R_0 \leq 1$. □

5.2. Global stability of infected equilibrium point.

Theorem 5.2. *E_1 is globally asymptotically stable if $R_0 > 1$*

Proof. We consider a Lyapunov function for $E_1 = (H*, I*, P*, V*)$

$$\begin{aligned} L(t) = & \left(1 + \frac{\alpha I^*}{\beta V^* H^*}\right)\left(H - H^* - H^* \ln\left(\frac{H}{H^*}\right)\right) \\ & + \frac{\alpha I^*}{\beta V^* H^*}\left(I - I^* - I^* \ln\left(\frac{I}{I^*}\right)\right) \\ & + \left(P - P^* - P^* \ln\left(\frac{P}{P^*}\right)\right) \\ & + \frac{\rho + \mu + \delta}{\rho}\left(V - V^* - V^* \ln\left(\frac{V}{V^*}\right)\right) \end{aligned}$$

Hence,

$$\begin{aligned}\frac{dL(t)}{dt} = &\left(1+\frac{\alpha I^*}{\beta V^* H^*}\right)\left(1-\frac{H^*}{H}\right)(s-rH-\beta VH)\\ &+\frac{\alpha I^*}{\beta V^* H^*}\left(1-\frac{I^*}{I}\right)(\beta VH-\delta I)\\ &+\left(1-\frac{P^*}{P}\right)(\beta VH+\alpha I-\mu_1 P)\\ &+\frac{\mu_1}{\rho}\left(1-\frac{V^*}{V}\right)(\rho P-cV)\end{aligned} \tag{16}$$

For the infected equilibrium point, the equation 16 can be simplified by the following equations:

$$s = rH*+\beta V*H*$$

$$\delta = \frac{\beta V*H*}{I*}$$

$$\mu_1 = \rho+\delta+\mu = \frac{\alpha I*+\beta V*H*}{P*}$$

$$c = \frac{\rho P*}{V*}$$

- The fist term:

$$T1 = \beta V*H*-\beta VH-\beta\frac{V*H*^2}{H}+\beta VH*+\alpha I*-\frac{\alpha I*VH}{V*H*}+\frac{\alpha I*H*}{H}+\frac{\alpha I*V}{V*}$$

- The second term:

$$T2 = \frac{\alpha I*VH}{V*H*}-\alpha I-\frac{\alpha I*^2 VH}{V*H*I}+\alpha I*$$

- The third term:

$$T3 = \beta VH-\frac{\beta V*H*P}{P*}-\frac{\beta VHP*}{P}+\beta V*H*+\alpha I-\frac{\alpha PI*}{P*}-\frac{\alpha IP*}{P}+\alpha I*$$

- The fourth term:

$$T4 = \frac{\beta V*H*P}{P*}-\beta VH*-\frac{\beta V*H*V*P}{P*}+\beta V*H*+\frac{\alpha I*P}{P*}-\frac{\alpha I*V}{V*}-\frac{\alpha I*V*P}{VP*}+\alpha I*$$

We obtain:

$$\begin{aligned}\frac{dL(t)}{dt} &= rH^*\left(1+\frac{\alpha I^*}{\beta V^*H^*}\right)\left(2-\frac{H}{H^*}-\frac{H^*}{H}\right)\\ &+\beta V^*H^*\left(3-\frac{H^*}{H}-\frac{V^*P}{P^*V}-\frac{VHP^*}{V^*H^*P}\right)\\ &+\alpha I^*\left(4-\frac{IP^*}{I^*P}-\frac{V^*P}{P^*V}-\frac{I^*VH}{V^*H^*I}-\frac{H^*}{H}\right)\end{aligned} \tag{17}$$

We have:

$$2-\frac{H}{H*}-\frac{H*}{H}\leq 0$$

$$3-\frac{H*}{H}-\frac{V*P}{P*V}-\frac{VHP*}{V*H*P}\leq 0$$

$$4-\frac{IP*}{I*P}-\frac{V*P}{P*V}-\frac{I*VH}{V*H*I}-\frac{H*}{H}\leq 0$$

Only at E_1 the derivative $\frac{dL(t)}{dt}=0$ and $\frac{dL(t)}{dt}<0$ at any other point. Then, E_1 is globally asymptotically stable if $R_0>1$ □

6. SIMULATION

To validate our theoretical findings, numerical simulations and discussions are presented here in this section using the value of the given parameter in the table:

Parameters	Figure 1	Figure 2	Figure 3	Figure 4	Figure 5	Figure 6	Figure 7
s	1	1	1	1	1	1	1
r	0.5	0.5	0.5	0.5	0.5	0.5	0.5
β	0.1	0.7	0.7	0.7	0.7	0.7	0.7
α	0.5	0.8	0.8	0.8	0.8	0.8	0.8
ρ	0.2	0.2	0.2	0.2	0.2	0.2	0.2
δ	0.8	0.3	0.3	0.3	0.3	0.3	0.3
μ	0.1	0.1	0.1	0.1	0.1	0.1	
c	0.3	0.3	0.3	0.3	0.3	0.3	0.3
ε_s	0	0	0.9	0.1	0.1	0.9	0.5
ε_α	0	0	0.9	0.1	0.9	0.1	0.5

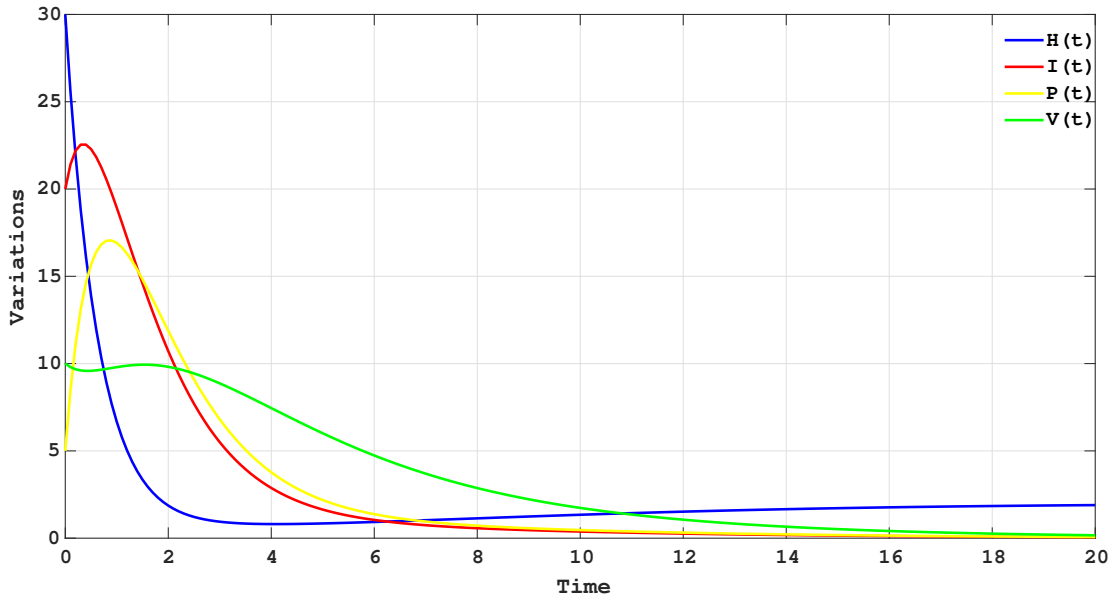

FIGURE 1. **Stability of the virus-free equilibrium point with:**

$R_0 = 0.197$, $E_0 = \{2,0,0,0\}$

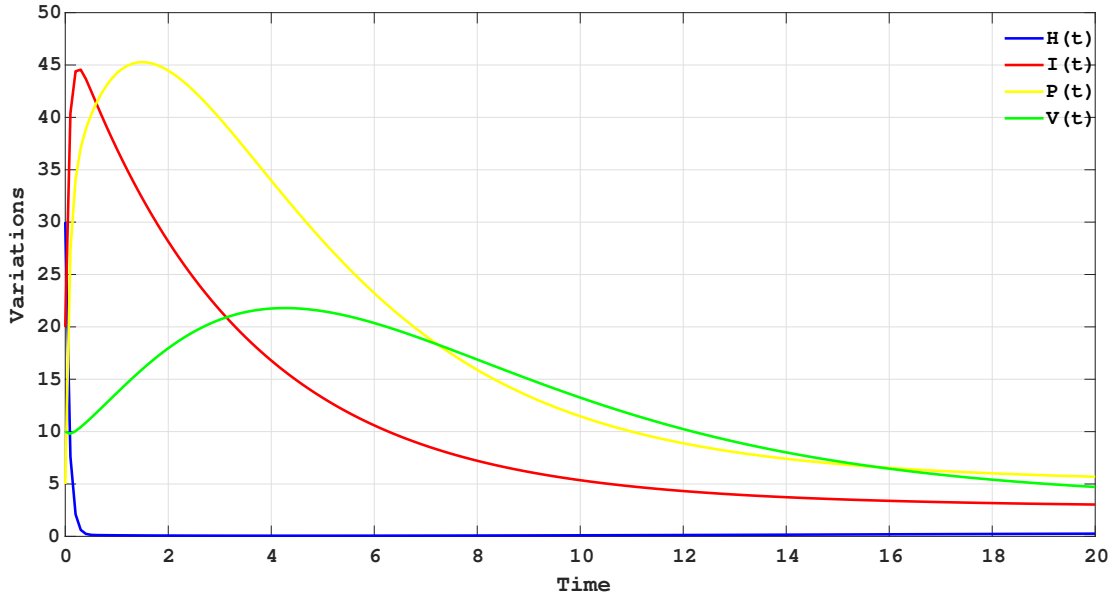

FIGURE 2. **Stability of the infected equilibrium point with:**

$R_0 = 5.703$, $E_1 = \{0.35,2.74,5.03,3.35\}$

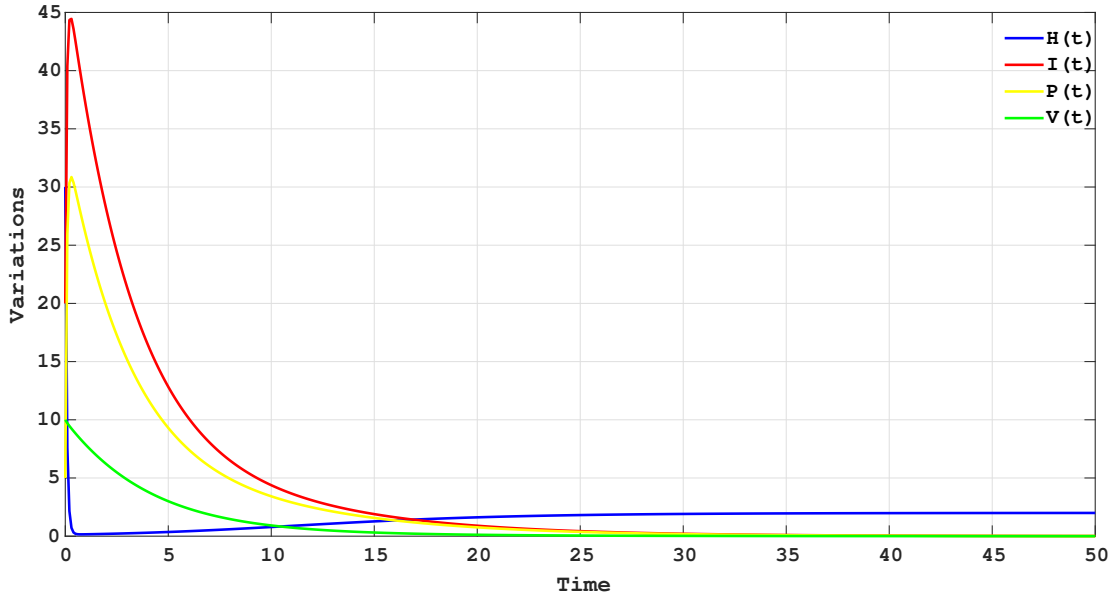

FIGURE 3. **Variation of the variables with medical treatment case with** :$R_0 = 5,703$, $\varepsilon_\alpha = 0,9$ and $\varepsilon_s = 0,9$

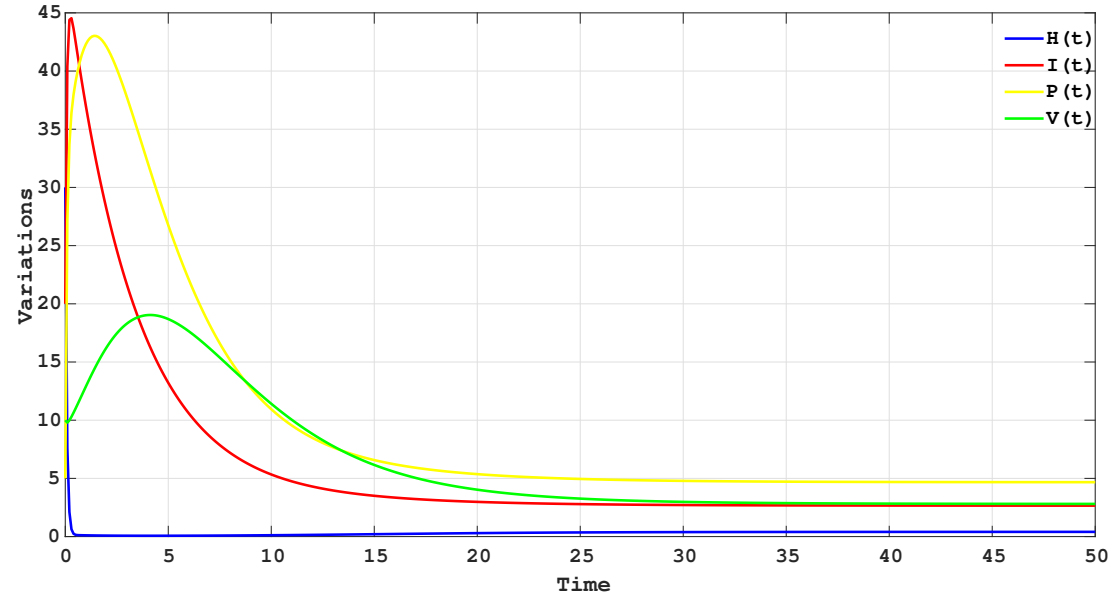

FIGURE 4. **Variation of the variables with medical treatment case with** :$R_0 = 5,703$, $\varepsilon_\alpha = 0,1$ and $\varepsilon_s = 0,1$

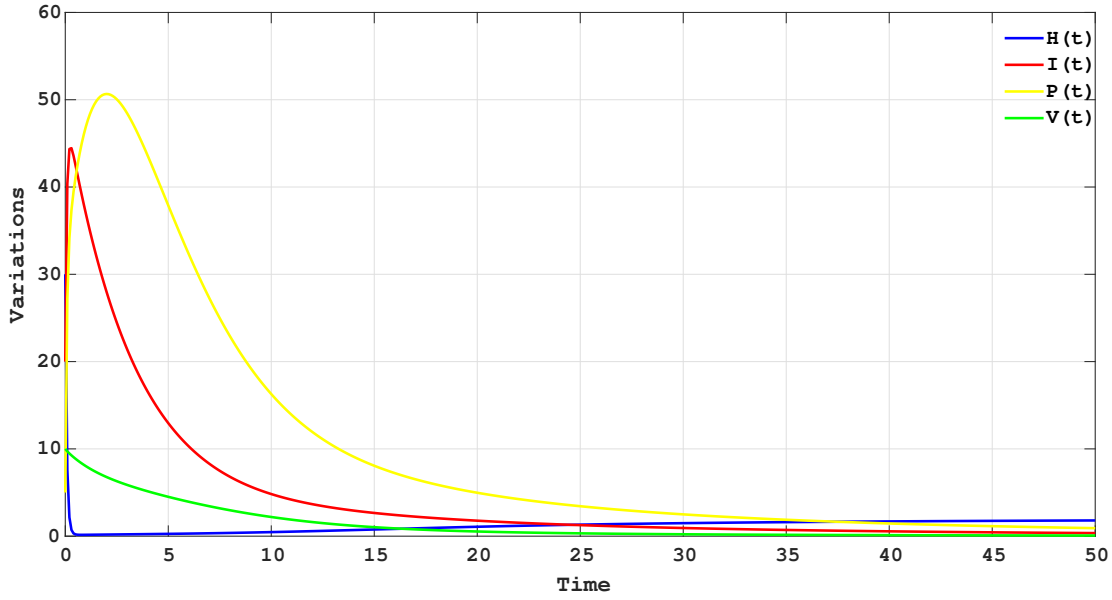

FIGURE 5. **Variation of the variables with medical treatment case with** :$R_0 = 5,703$, $\varepsilon_\alpha = 0,9$ and $\varepsilon_s = 0,1$

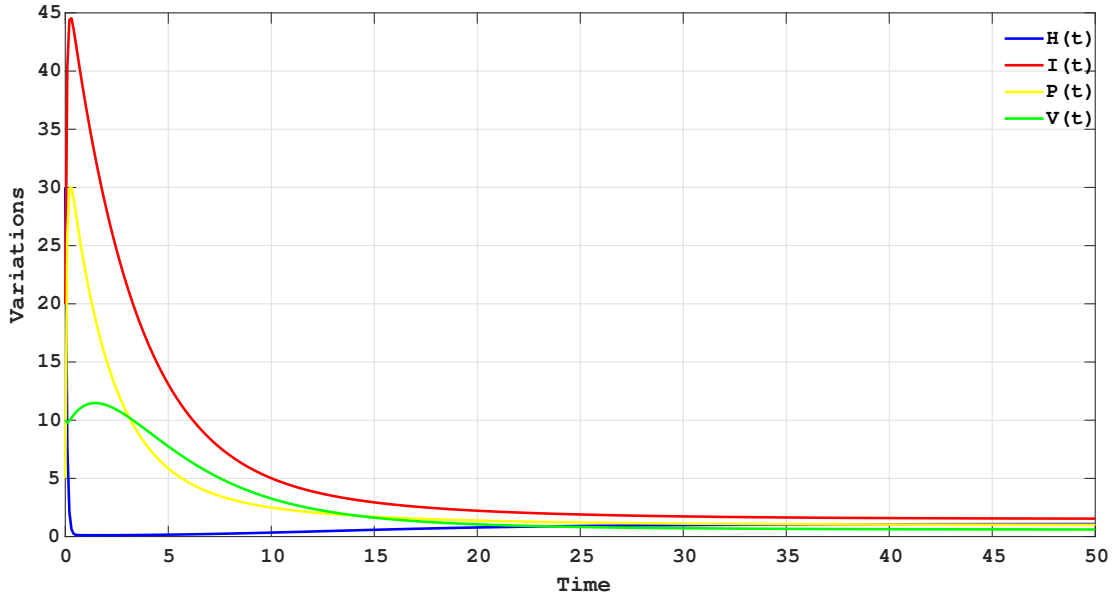

FIGURE 6. **Variation of the variables with medical treatment case with** :$R_0 = 5,703$, $\varepsilon_\alpha = 0,1$ and $\varepsilon_s = 0,9$

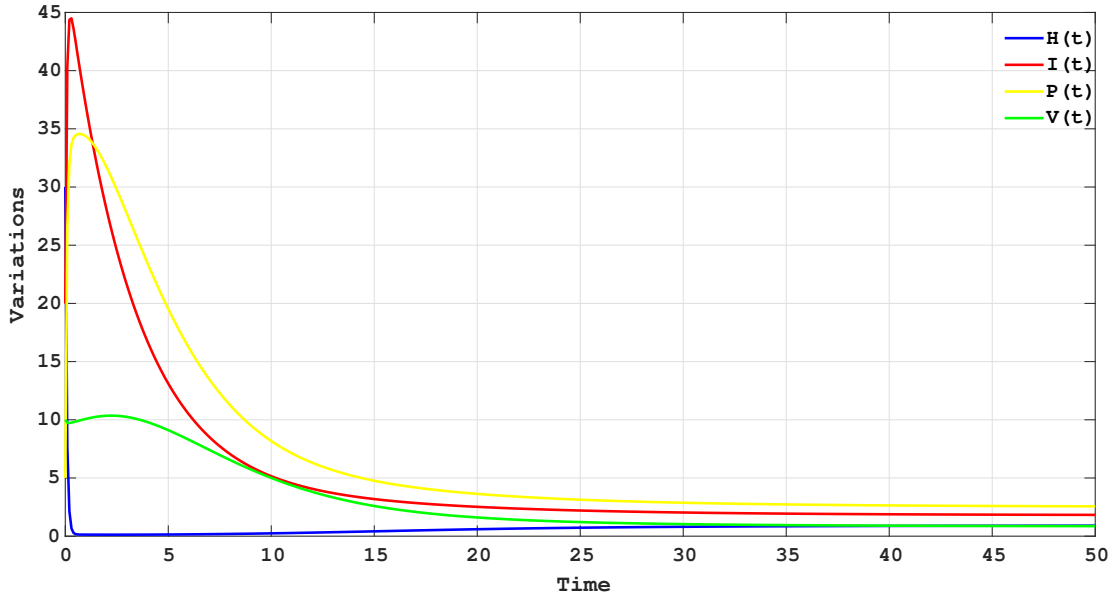

FIGURE 7. **Variation of the variables with medical treatment case with** :$R_0 = 5,703$, $\varepsilon_\alpha = 0,5$ and $\varepsilon_s = 0,5$

We see in figure 1 that all curves decrease towards 0 except that of the target cells that converge well towards our equilibrium point corresponding to $R_0 = 0.197$ which confirms our result given in theorem 2 for the global stability of free virus equilibrium. On the other hand, regarding the second equilibrium point, figure 2 clearly shows that all the curves converge towards this equilibrium point. Because in this case the basic reproduction number is larger than 1 with the same initial conditions considered in Figure 1. Therefore, the theorem 3 which was well confirmed by this numerical simulation resulted in the same result. In the case of treatment, we see in figure 3 that all the curves rapidly decrease to zero with a high efficiency of the treatment considered and that the Target cells return to their stability even if the basic reproduction rate is very high $R_0 = 5,703$, which means the importance of treatment in reducing infection. But in the figure 4, the efficiency of the treatment is low which causes a less significant decrease in the curves of $I(t)$, $P(t)$ and $V(t)$ even if they stabilize from a certain time (between 20 and 25 days). With increased efficiency of responsible treatment to block intracellular viral production, we notice in the figure 5 that the number of viruses takes to tend to zero in a shorter time in the first ten days, the other curves tend to zero after the 40th day and the target cells return to

stabilize after they disappear in the first days of infection while the total number of intracellular viral RNA reaches its peak within the first 5 days. On the other hand, in the figure 6, we increase the efficiency of the treatment responsible for blocking the assembly or secretion of the virion, the curve representing $P(t)$ arrives at a peak less and faster then tends to zeros. However, if we consider an efficiency of 0.5 for both treatments, we note in figure 7that the curves of P and V take time to reach its peak and slowly return to reach zero taking a long time only in figure 6 without noticing a significant change in the variations of infected cells.

7. Conclusion

In this paper, we analyzed a new multiscale HBV model with therapy. The model contained four compartments; Target cells, infected cells, intracellular viral pgRNA pooled in all infected cells and viruses. We started our analysis by defining the conditions of the existence, positivity of solutions. The model have two equilibrium point, the first is a virus-free equilibrium point and the second is the infected equilibrium point. For the basic reproduction number, we used an approach that is based in the new generation method. By using of two candidates Lyapunov functions, we could give the global stability of the different equilibrium point. As a result, if the basic reproduction number is less than 1, the virus-free equilibrium is asymptotically globally stable, while the stability of the infected equilibrium point is established if $R_0 > 1$. Numerical simulation is given as a validation of the theoretical results and give us a view about efficiency of the treatment.

Conflict of Interests

The author(s) declare that there is no conflict of interests.

References

[1] World Health Organization, Prevention and Control of Viral Hepatitis Infection: Framework for Global Action, WHO/HSE/PED/HIP/GHP 2012.1, World Health Organization, 2012. https://www.who.int/publications/i/item/prevention-and-control-of-viral-hepatitis-infection-framework-for-global-action.

[2] M. Jefferies, B. Rauff, H. Rashid, T. Lam, S. Rafiq, Update on Global Epidemiology of Viral Hepatitis and Preventive Strategies, World J. Clin. Cases 6 (2018), 589–599. https://doi.org/10.12998/wjcc.v6.i13.589.

[3] E. Franco, B. Bagnato, M.G. Marino, C. Meleleo, L. Serino, L. Zaratti, Hepatitis B: Epidemiology and Prevention in Developing Countries, World J. Hepatol. 4 (2012), 74–80. https://doi.org/10.4254/wjh.v4.i3.74.

[4] S.K. Sharma, N. Saini, Y. Chwla, Hepatitis B Virus: Inactive Carriers, Virol. J. 2 (2005), 82. https://doi.org/10.1186/1743-422x-2-82.

[5] J. Summers, W.S. Mason, Replication of the Genome of a Hepatitis B-Like Virus by Reverse Transcription of an RNA Intermediate, Cell 29 (1982), 403–415. https://doi.org/10.1016/0092-8674(82)90157-x.

[6] J. Summers, A. O'Connell, I. Millman, Genome of Hepatitis B Virus: Restriction Enzyme Cleavage and Structure of DNA Extracted from Dane Particles, Proc. Natl. Acad. Sci. U.S.A. 72 (1975), 4597–4601. https://doi.org/10.1073/pnas.72.11.4597.

[7] J.A. Sohn, S. Litwin, C. Seeger, Mechanism for CCC DNA Synthesis in Hepadnaviruses, PLoS One 4 (2009), e8093. https://doi.org/10.1371/journal.pone.0008093.

[8] J.S. Tuttleman, C. Pourcel, J. Summers, Formation of the Pool of Covalently Closed Circular Viral DNA in Hepadnavirus-Infected Cells, Cell 47 (1986), 451–460. https://doi.org/10.1016/0092-8674(86)90602-1.

[9] R.C. Hirsch, J.E. Lavine, L.-J. Chang, H.E. Varmus, D. Ganem, Polymerase Gene Products of Hepatitis B Viruses Are Required for Genomic RNA Packaging as Well as for Reverse Transcription, Nature 344 (1990), 552–555. https://doi.org/10.1038/344552a0.

[10] J. Summers, P.M. Smith, A.L. Horwich, Hepadnavirus Envelope Proteins Regulate Covalently Closed Circular DNA Amplification, J. Virol. 64 (1990), 2819–2824. https://doi.org/10.1128/jvi.64.6.2819-2824.1990.

[11] J.E. Newbold, H. Xin, M. Tencza, G. Sherman, J. Dean, S. Bowden, S. Locarnini, The Covalently Closed Duplex Form of the Hepadnavirus Genome Exists in Situ as a Heterogeneous Population of Viral Minichromosomes, J. Virol. 69 (1995), 3350–3357. https://doi.org/10.1128/jvi.69.6.3350-3357.1995.

[12] M. Pasek, T. Goto, W. Gilbert, B. Zink, H. Schaller, P. MacKay, G. Leadbetter, K. Murray, Hepatitis B Virus Genes and Their Expression in E. coli, Nature 282 (1979), 575–579. https://doi.org/10.1038/282575a0.

[13] A. Krause, U. Haberkorn, W. Mier, Strategies for the Treatment of HBV/HDV, Eur. J. Pharmacol. 833 (2018), 379–391. https://doi.org/10.1016/j.ejphar.2018.06.030.

[14] O. Khyar, A. Meskaf, K. Allali, Mathematic Analysis of a SIHV COVID-19 Pandemic Model Taking into Account a Vaccination Strategy, in: R.P. Mondaini, (ed) Trends in Biomathematics: Stability and Oscillations in Environmental, Social, and Biological Models, Springer, Cham, pp. 211–223, (2022). https://doi.org/10.1007/978-3-031-12515-7_11.

[15] Z. Yaagoub, K. Allali, Global Stability of Multi-Strain SEIR Epidemic Model with Vaccination Strategy, Math. Comput. Appl. 28 (2023), 9. https://doi.org/10.3390/mca28010009.

[16] Y. Tabit, A. Meskaf, K. Allali, Mathematical Analysis of HIV Model with Two Saturated Rates, CTL and Antibody Responses, World J. Model. Simul. 12 (2016), 136–145.

[17] I. Aamoum, A. Meskaf, Z. Yaagoub, E.M. Farah, Mathematical Analysis of a Fractional-Order Influenza Model with Resistant and Non-Resistant Strains, Iran. J. Numer. Anal. Optim. 16 (2026), 703–726. https://doi.org/10.22067/ijnao.2026.96816.1791.

[18] M.A. Nowak, S. Bonhoeffer, A.M. Hill, R. Boehme, H.C. Thomas, H. McDade, Viral Dynamics in Hepatitis B Virus Infection, Proc. Natl. Acad. Sci. U.S.A. 93 (1996), 4398–4402. https://doi.org/10.1073/pnas.93.9.4398.

[19] A. Murase, T. Sasaki, T. Kajiwara, Stability Analysis of Pathogen-Immune Interaction Dynamics, J. Math. Biol. 51 (2005), 247–267. https://doi.org/10.1007/s00285-005-0321-y.

[20] S. Hews, S. Eikenberry, J.D. Nagy, Y. Kuang, Rich Dynamics of a Hepatitis B Viral Infection Model with Logistic Hepatocyte Growth, J. Math. Biol. 60 (2010), 573–590. https://doi.org/10.1007/s00285-009-0278-3.

[21] V.-A. Sypsa, K. Mimidis, N.C. Tassopoulos, D. Chrysagis, T. Vassiliadis, A. Moulakakis, M. Raptopoulou, C. Haida, A. Hatzakis, A Viral Kinetic Study Using Pegylated Interferon Alfa-2b and/or Lamivudine in Patients with Chronic Hepatitis B/HBeAg Negative, Hepatology 42 (2005), 77–85. https://doi.org/10.1002/hep.20738.

[22] A. Meskaf, K. Allali, Optimal Control of a Delayed Hepatitis B Viral Infection Model with DNA-Containing Capsids and Cure Rate, in: R.P. Mondaini, (ed) Trends in Biomathematics: Mathematical Modeling for Health, Harvesting, and Population Dynamics, Springer, Cham, pp. 23–33, (2019). https://doi.org/10.1007/978-3-030-23433-1_2.

[23] S.A. Gourley, Y. Kuang, J.D. Nagy, Dynamics of a Delay Differential Equation Model of Hepatitis B Virus Infection, J. Biol. Dyn. 2 (2008), 140–153. https://doi.org/10.1080/17513750701769873.

[24] G. Huang, Y. Takeuchi, W. Ma, Lyapunov Functionals for Delay Differential Equations Model of Viral Infections, SIAM J. Appl. Math. 70 (2010), 2693–2708. https://doi.org/10.1137/090780821.

[25] B.-Z. Guo, L.-M. Cai, A Note for the Global Stability of a Delay Differential Equation of Hepatitis B Virus Infection, Math. Biosci. Eng. 8 (2011), 689–694. https://doi.org/10.3934/mbe.2011.8.689.

[26] K. Wang, W. Wang, S. Song, Dynamics of an HBV Model with Diffusion and Delay, J. Theor. Biol. 253 (2008), 36–44. https://doi.org/10.1016/j.jtbi.2007.11.007.

[27] S.M. Ciupe, R.M. Ribeiro, P.W. Nelson, A.S. Perelson, Modeling the Mechanisms of Acute Hepatitis B Virus Infection, J. Theor. Biol. 247 (2007), 23–35. https://doi.org/10.1016/j.jtbi.2007.02.017.

[28] Q. Li, F. Lu, G. Deng, K. Wang, Modeling the Effects of Covalently Closed Circular DNA and Dendritic Cells in Chronic HBV Infection, J. Theor. Biol. 357 (2014), 1–9. https://doi.org/10.1016/j.jtbi.2014.04.037.

[29] L. Rong, J. Guedj, H. Dahari, D.J. Coffield, M. Levi, P. Smith, A.S. Perelson, Analysis of Hepatitis C Virus Decline during Treatment with the Protease Inhibitor Danoprevir Using a Multiscale Model, PLoS Comput. Biol. 9 (2013), e1002959. https://doi.org/10.1371/journal.pcbi.1002959.

[30] L. Rong, A.S. Perelson, Mathematical Analysis of Multiscale Models for Hepatitis C Virus Dynamics under Therapy with Direct-Acting Antiviral Agents, Math. Biosci. 245 (2013), 22–30. https://doi.org/10.1016/j.mbs.2013.04.012.

[31] K. Kitagawa, S. Nakaoka, Y. Asai, K. Watashi, S. Iwami, A PDE Multiscale Model of Hepatitis C Virus Infection Can Be Transformed to a System of ODEs, J. Theor. Biol. 448 (2018), 80–85. https://doi.org/10.1016/j.jtbi.2018.04.006.

[32] J. Guedj, H. Dahari, L. Rong, N.D. Sansone, R.E. Nettles, S.J. Cotler, T.J. Layden, S.L. Uprichard, A.S. Perelson, Modeling Shows That the NS5A Inhibitor Daclatasvir Has Two Modes of Action and Yields a Shorter Estimate of the Hepatitis C Virus Half-Life, Proc. Natl. Acad. Sci. U.S.A. 110 (2013), 3991–3996. https://doi.org/10.1073/pnas.1203110110.

[33] C. Castillo-Chavez, Z. Feng, W. Huang, On the Computation of R_0 and Its Role on Global Stability, in: C. Castillo-Chavez, S. Blower, P. van den Driessche, D. Kirschner, A.A. Yakubu, (eds) Mathematical Approaches for Emerging and Reemerging Infectious Diseases: An Introduction, The IMA Volumes in Mathematics and its Applications, Springer, New York, pp. 229–250, (2002). https://doi.org/10.1007/978-1-4757-3667-0_13.

[34] T. Kajiwara, T. Sasaki, Y. Takeuchi, Construction of Lyapunov Functionals for Delay Differential Equations in Virology and Epidemiology, Nonlinear Anal. Real World Appl. 13 (2012), 1802–1826. https://doi.org/10.1016/j.nonrwa.2011.12.011.

[35] J. Danane, K. Allali, Z. Hammouch, Mathematical Analysis of a Fractional Differential Model of HBV Infection with Antibody Immune Response, Chaos Solit. Fractals 136 (2020), 109787. https://doi.org/10.1016/j.chaos.2020.109787.

[36] K. Allali, A. Meskaf, A. Tridane, Mathematical Modeling of the Adaptive Immune Responses in the Early Stage of the HBV Infection, Int. J. Differ. Equ. 2018 (2018), 1–13. https://doi.org/10.1155/2018/6710575.

[37] A. Meskaf, Y. Tabit, K. Allali, Global Analysis of a HCV Model with CTL, Antibody Responses and Therapy, Appl. Math. Sci. 9 (2015), 3997–4008. https://doi.org/10.12988/ams.2015.54334.

[38] A. Meskaf, K. Allali, Y. Tabit, Optimal Control of a Delayed Hepatitis B Viral Infection Model with Cytotoxic T-Lymphocyte and Antibody Responses, Int. J. Dyn. Control 5 (2017), 893–902. https://doi.org/10.1007/s40435-016-0231-4.

[39] J. Danane, A. Meskaf, K. Allali, Optimal Control of a Delayed Hepatitis B Viral Infection Model with HBV DNA-Containing Capsids and CTL Immune Response, Optim. Control Appl. Methods 39 (2018), 1262–1272. https://doi.org/10.1002/oca.2407.

[40] A. Meskaf, M. Elkaf, K. Allali, Viral Infection Dynamics of HBV DNA-Containing Capsids with Logistics Growth and Saturated Rate, Commun. Math. Biol. Neurosci. 2023 (2023), 7. https://doi.org/10.28919/cmbn/7842.

[41] Z. Yaagoub, J. Danane, K. Allali, On a Two-Strain Epidemic Mathematical Model with Vaccination, Comput. Methods Biomech. Biomed. Eng. 27 (2024), 632–650. https://doi.org/10.1080/10255842.2023.2197542.

[42] A. Meskaf, O. Khyar, J. Danane, K. Allali, Global Stability Analysis of a Two-Strain Epidemic Model with Non-Monotone Incidence Rates, Chaos Solit. Fractals 133 (2020), 109647. https://doi.org/10.1016/j.chaos.2020.109647.